



Analysis of the Simulation Results of Three Carbon Dioxide (CO₂) Cycle Models

Antero Ollila^{1*}

¹*Department of Civil and Environmental Engineering (Emer.), School of Engineering, Aalto University, Espoo, Otakaari 1, Box 11000, 00076 AALTO, Finland.*

Author's contribution

The sole author designed, analysed, interpreted and prepared the manuscript.

Article Information

DOI: 10.9734/PSIJ/2019/v23i430168

Editor(s):

(1) Dr. Lei Zhang, Assistant Professor of Physics, Winston-Salem State University, Winston Salem, North Carolina 27110, USA.

(2) Dr. Roberto Oscar Aquilano, School of Exact Science, National University of Rosario (UNR), Rosario Physics Institute (IFIR CONICET-UNR), Argentina.

Reviewers:

(1) Agu Eensaar, Tallinn University of Applied Sciences, Estonia.

(2) Rafael Infante, Caribbean University, Puerto Rico.

Complete Peer review History: <http://www.sdiarticle4.com/review-history/53980>

Received 10 November 2019

Accepted 15 January 2020

Published 20 January 2020

Original Research Article

ABSTRACT

The CO₂ (carbon dioxide) circulation models referred by the IPCC (Intergovernmental Panel on Climate Change) show that the increase of atmospheric CO₂ by 240 GtC (Gigatonnes of carbon) from 1750 to 2011 is totally anthropogenic in nature, which corresponds to the permille value of about -12.5‰, but the observed value is only -8.3‰. The author's improved 1DAOBM-3 CO₂ circulation model shows that the anthropogenic CO₂ amount in 2011 is only 73 GtC, satisfying the observed atmospheric permille values from 1750 to 2017. The CO₂ circulation between the ocean and the atmosphere has increased the amount of atmospheric CO₂ by natural CO₂ 197 GtC from the ocean, and this explains why the net uptake rate is only 1.9 GtC yr⁻¹. Together with the anthropogenic amount of 73 GtC, the total increase is 270 GtC by 2017, corresponding to the observed atmospheric CO₂ concentration. The simulations for 1000 GtC emissions by 2100 have been carried out by three models, including 1DAOBM-3, Bern2.5CC, and the mean model of 15 circulation models (called Joos 2013). The residence time of 1DAOBM-3 is 16 years for anthropogenic CO₂ impulse, the same as for the radiocarbon decay time. The decay time of 1DAOBM-3 for the impulse function is about 600 years meaning the residence time of about 150 years only. These values are much shorter than the residence times of two other models, which show that 25±9‰ of any anthropogenic CO₂ is still found in the atmosphere after 1,000 years. The

*Corresponding author: E-mail: aveollila@yahoo.com;

reasons have been analyzed. The advantage of 1DAOBM-3 over the other models is that its results are in line with the oceanic and atmospheric observations from 1750 to 2017 but the future simulations include uncertainties due to ocean and biosphere uptake rate models.

Keywords: Climate change; lifetime of atmospheric CO₂; CO₂ cycle models; climate models.

1. INTRODUCTION

CO₂ cycle models are applied to calculate and evaluate the lifetime of atmospheric CO₂ caused by the anthropogenic emissions into the atmosphere. The IPCC has selected the Bern Carbon cycle model (Bern 2.5 CC) in the Assessment Report 4 (AR4) to describe the dynamic responses of the anthropogenic CO₂ perturbations [1,2]. In the AR5 report, the IPCC [3] has stated that “the removal of human-emitted CO₂ from the atmosphere by natural processes will take a few hundred thousand years [high confidence]. Depending on the RCP scenario considered, about 15 to 40% of emitted CO₂ will remain in the atmosphere longer than 1,000 years.” These lifetime values are based on the CO₂ cycle model by Joos et al. [4]. Ollila [5] has introduced an enhanced semi-empirical atmosphere-ocean-biosphere model by the name 1DAOBM-2, which gives much shorter lifetimes: the residence time (T) of the anthropogenic CO₂ is 16 years and the residence time of the total CO₂ is 55 years. It should be noted that the term “lifetime” is the same quantity as “relaxation time” or “adjustment time,” which is about four times longer than the residence time.

One objective of this study is to introduce the enhanced version of 1DAOBM-3 and the simulation results of the model. Another objective is to analyze and compare the simulation results of these three CO₂ cycle models, 1DAOBM-3, BernCC2.5, and Joos2013 [4]. A very decisive feature of the 1DAOBM-3 in comparison to the other two models is its distinct difference between anthropogenic CO₂, natural CO₂, and the mixture of these two CO₂ types, named “total CO₂.” This feature turns out to be an important factor in the validation of results.

In the research studies [2,4], there is a serious deficiency or error concerning anthropogenic CO₂. Joos et al. [2] state that “Currently, only about half of the anthropogenic CO₂ emission stays airborne.” In Joos et al. [4], there is a reference to the Impulse Response Function (IRF): “The IRF is thus a first order approximation how excess anthropogenic carbon is removed from the atmosphere by a particular

model.” The researchers use the terms “anthropogenic CO₂” and “atmospheric CO₂” as if they were the same concepts, which they are not, because atmospheric CO₂ is a mixture of anthropogenic and natural CO₂. In AR5, the IPCC [3] (p. 467) refers to the study of Joos et al. [4] in pointing to the atmospheric CO₂ increase: “About half of the emissions remained in the atmosphere 240 PgC±10 PgC since 1750.”

According to Joos et al. [4] the whole increase of the atmospheric CO₂ since 1750 is anthropogenic. Huge dissolving rate 80±20% GtC yr⁻¹ flushes CO₂ from the atmosphere into the ocean and at the same time about the same size absorbing rate releases CO₂ from the ocean into the atmosphere. The anthropogenic CO₂ amount was zero in the surface layer of the ocean in 1750 and still, its proportional content is still much lower than in the atmosphere. It means that the natural CO₂ flux from the ocean compensates the anthropogenic CO₂ loss into the ocean. It looks like that this natural CO₂ has not been considered in the model of [4].

1DAOBM-3 applies the same equation as 1DAOBM-2 for calculating the accurate permille value of the atmospheric CO₂ composition and it is calculated using the actual atmospheric CO₂ amounts (GtC)

$$\delta^{13}\text{C} = (\text{CIA}_{\text{ant}} * (-28) + (\text{CIA}_{\text{tot}} - \text{CIA}_{1750} - \text{CIA}_{\text{ant}}) * (-8) + \text{CIA}_{1750} * (-6.35)) / \text{CIA}_{\text{tot}} \quad (1)$$

where CIA_{ant} is anthropogenic CO₂, CIA_{tot} is the total CO₂, and CIA₁₇₅₀ is the total CO₂ in 1750. The measurement unit of ¹³C proportion is δ¹³C and it is a fraction of carbon isotope 13 expressed as (‰) (written also in forms per mil, per mill, permil, permil or permille). Equation (1) shows that the contemporary atmosphere is the mixture of three CO₂ fractions: the anthropogenic amount, the fraction originating from the ocean, and the atmospheric mass in 1750. The permille values of these fractions are: the fossil fuel CO₂ - 28 ‰, the ocean -8 ‰, and the atmosphere in 1750 -6.35 ‰ [6,7]. The ¹³C/¹²C in equation (1) is 0.011162 for natural CO₂ and 0.010922 for anthropogenic CO₂. There is a light fractionation, when CO₂ passes through the air/sea interface.

Inoue et al. [8] have estimated that air to sea value is about -10‰ and the sea to air value is -8‰, and therefore the latter value is used in equation (1) for the CO₂ flux originating from the ocean. The calculated value of 1DAOBM-2 using equation (1) is -8.35‰ for 2011, which is the same as the observed permille value in 2011 [9].

The Joos2013 model found that the amount of anthropogenic CO₂ is 240 GtC when the total atmospheric CO₂ amount of 835 GtC in 2011 would mean the portion is 28.8% for the anthropogenic CO₂. Applying these values in equation (1) gives the permille value -12.45‰. This enormous error of Joos2013 model can be also illustrated with a graphical presentation.

A calculation formula for permille value is

$$\delta^{13}\text{C} = ((^{13}\text{C}/^{12}\text{C})_{\text{sample}} / (^{13}\text{C}/^{12}\text{C})_{\text{standard}} - 1) * 1000 \quad (2)$$

where $(^{13}\text{C}/^{12}\text{C})_{\text{sample}}$ is the actual isotope relationship of a CO₂ fraction in question. The value of $(^{13}\text{C}/^{12}\text{C})_{\text{standard}}$ is 0.0112372. It means that permille value depends linearly on the $^{13}\text{C}/^{12}\text{C}$ and they are depicted in Fig. 1 according to equation (2).

The hypothetical permille value of Joos2013 is the same as the observed permille value but this value is not according to the linear dependency of $^{13}\text{C}/^{12}\text{C}$ as it should be. An analysis for

1DAOBM-2 and Joos2013 was carried using these values and the results are depicted in Table 1.

This analysis gives permille value of -12.84‰ for the atmosphere according to Joos2013 composition and the difference is insignificant with respect to the -12.45‰. The atmosphere according to Joos2013 could reach the observed permille value of -8.35‰ only if the permille value of the natural CO₂ fraction would be -0.29‰. There is no such a CO₂ phase on the Earth.

The simplest way to calculate the atmospheric permille value is by adding together the anthropogenic CO₂ and the natural CO₂ according to their proportions in the atmosphere in 2011: $\delta^{13}\text{C} = 0.29*(-28) + 0.71*(-6.35) = -12.57\text{‰}$. One could criticize the permille value -6.35‰ of the natural CO₂ in this calculation. It might have increased during the centuries but in that case, the permille value difference of the Joos2013 to the observed permille value would be even greater.

The gap between these calculated and observed permille values of Joos2013 is huge and shows that Bern2.5CC and Joos2013 have a prominent error in their model constructions. This great error creates a justified concern about whether the overall results of these models are based on

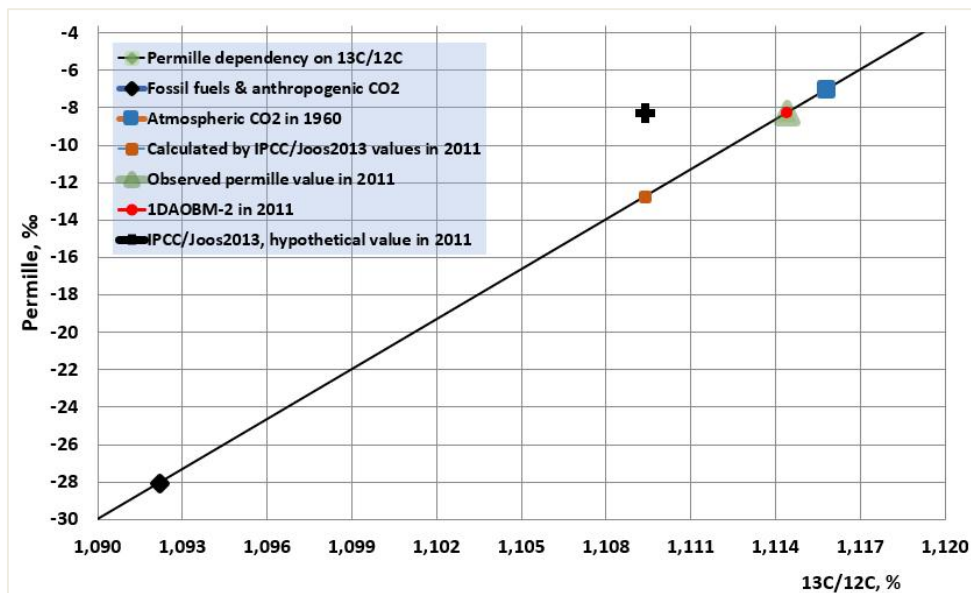


Fig. 1. The permille values of different CO₂ compounds as a function of $^{13}\text{C}/^{12}\text{C}$

Table 1. Permille values for 1DAOBM-2 and Joos2012 results in 2011

	Atmosphere 2011		1DAOBM-3		
	GtC	13C/12C	12C, GtC	13C, GtC	Permille, ‰
Natural CO ₂	771	0,011162	762,489	8,510	-6,35
Anthropogenic CO ₂	63	0,010922	62,3193	0,680	-28
Total CO ₂	834	0,011144	824,808	9,191	-8,31
Joos2013 and the IPCC					
Natural CO ₂	594	0,011162	587,443	6,557	-6,35
Anthropogenic CO ₂	240	0,010922	237,407	2,592	-28
Total CO ₂	834	0,011093	824,850	9,149	-12,84

real grounds. The deficiency of these two models may be one reason the researchers of these studies do not refer to the atmospheric permille value or why they do not use it for the calibration or the validation.

There are two schools of thought about the ocean's capacity to dissolve the atmospheric CO₂ and at which rate this dissolution can happen. The most common approach could be called the "buffer factor"-based estimation, or the buffering of the CO₂ exchange from air to seawater, also known as the "Revelle factor" [10]. The Revelle factor value is about 14 in the high latitude waters and about 10 in equatorial waters. Buffer factor 10 means that a 10% increase of partial CO₂ pressure can increase only 1% of the total carbon amount in the ocean. This approach has led to the maximum net dissolving rate of 2.2 GtCyr⁻¹ by [11], 2.3 GtC yr⁻¹ by [12], and 2.3±0.6 GtC yr⁻¹ by [13], which will not increase despite an increased atmospheric CO₂ concentration. The Bern2.5CC and Joos2013 models apply the buffer capacity approach.

There are studies that do not accept the almost constant buffer capacity of the ocean. The increased atmospheric CO₂ concentration can increase the buffer capacity by 2.5 to 6 times [14]. Other minerals like borate, kaolinite, and clay minerals can essentially increase the storage capacity of CO₂ [15,16], and in the latter study, the researchers have concluded that these buffers together mean an infinite buffer capacity. In 1DAOBM, the dissolution rate is not restricted by the buffer factor estimate.

2. METHODS

2.1 The Carbon Cycle Model 1DAOBM and Its Improvements

Ollila [17] introduced the 1DAOBM-1 model in 2015 and an improved version, 1DAOBM-2, a year later [5]. The 1DAOBM is a four-box model

in which the ocean is divided into surface ocean and the intermediate and deep ocean. 1DAOBM contains two ideal mixing components (the atmosphere and the ocean), one plug flow component with four parallel residence times (the biosphere), and the outlet (the intermediate & deep ocean). The oceans have been assumed to have the capacity to dissolve the anthropogenic CO₂ emissions of the present century. The surface ocean part is based on the known dissolution chemical equations. The net flux rate from the surface ocean into the deep ocean is based on the empirical data. The removal of the anthropogenic CO₂ from the atmosphere is based on the huge carbon cycle flux rates of the dissolution pump and the biosphere carbon cycle, which remove 20–25% of CO₂ yearly from the atmosphere to other reservoirs and, at the same time, recycle natural and anthropogenic carbon.

An important feature of 1DAOBM is its capability to keep separated anthropogenic CO₂, natural CO₂, and their mixture, total CO₂. This feature cannot be found in the other two models used in the simulation studies.

2.2 Improvements in the Carbon Cycle Model 1DAOBM-3

The improvements of the 1DAOBM-3 model have been explained in Appendix. The calibrations of 1DAOBM-3 are now based on the measurements in the atmosphere because they are much more accurate in comparison to the oceanic CO_{2,ant} measurements. The permille values from the Scripps data set [9], the CO₂ emission data are provided by CDIAC [18], and the ocean temperature data originate from NOAA [19].

2.3 Simulations Results by 1DAOBM-3

The simulation results of the CO₂ fluxes and amounts in the reservoirs by 1DAOBM-2 have been repeated by 1DAOBM-3. The dissolving rate by the surface ocean depends strongly on

the temperature according to Henry's law. In simulations up to 2013, the coefficient of determination is $r^2 = 0.83$ when the Pinatubo anomaly was removed. The decay rate simulation applying 1DAOBM-3 for 1964–2017 gives a similar residence time of 16 years for anthropogenic CO₂, as in the earlier simulation for 1960–2013. This simulation is almost exactly in line with the radiocarbon ¹⁴C decay rate starting in 1964 when the nuclear tests in the atmosphere were suspended [5]. The radiocarbon is a perfect tracer to analyze the dynamic behavior of anthropogenic CO₂ because both CO₂ isotope ¹³C and ¹⁴C fluxes start from zero in the CO₂ circulation system. Because the radiocarbon has been in the descending mode for decades, it is not applicable for showing the actual dynamic behavior of CO₂ concentration in the ocean, but it is an excellent tracer in the atmosphere. Fig. 2 depicts the results of simulation using the real emission values, the observed sea temperatures, the calculated CO₂ fluxes, and the calculated/observed CO₂ concentrations.

Although the emissions increase, the calculated net anthropogenic CO₂ flux rate into the atmosphere remains relatively low; on the other hand, the natural CO₂ flux from the ocean into the atmosphere increases continuously. The reasons for these values are analyzed in the validation section. It might look odd that the yearly net anthropogenic flux $FB_{ant,dn}$ into the biosphere can be even higher than a yearly emission value, as it is shown during 1900–1970. This is because the $FB_{ant,dn}$ depends on the actual CO₂ amount in the atmosphere and not on the yearly emission flux values.

The cumulative CO₂ flux changes and reservoir change values from 1750 to 2017 are depicted in Fig. 3.

The major observation of this model simulation is that the amount of anthropogenic CO₂ in the atmosphere is only 73 GtC in 2017, but the natural CO₂ originating from the ocean is 197 GtC. This means that the total CO₂ increase in the ocean is only 36 GtC from 1750 to 2017. The CO₂ land sink in 2017 is 2.8 GtC yr⁻¹ being close to the estimate 2.5±1.3 of the IPCC [3] (p. 486) for 2002–2011. The sequestration capacity of the ocean has almost not been utilized. The division of the anthropogenic CO₂ between the biosphere (127 GtC) and the ocean (234 GtC) is 35% versus 65% by 2017. Sabine et al. [20] have estimated that the anthropogenic CO₂ sink value

of 120 GtC in 1994 is about 30% the maximum sink capacity of the ocean, thus giving a maximum sink capacity value of 400 GtC.

2.4 Validation of Simulation Results

The validation of 1DAOBM-3 can be tested in four different ways. Firstly, Sabine et al. [20] have found that the global oceanic anthropogenic CO₂ sink from the period of 1800 to 1994 is 118±19 GtC, the estimate of Waugh et al. [21] is 134 GtC for the same period, and Khatiwala et al. [13] value for the inventory is 140±25 GtC. Sabine and Tanhua [22] summarized that the most common estimate of the oceanic anthropogenic CO₂ inventory in the mid-1990s is about 120 GtC. The model-calculated value for 1994 is 123 GtC, which is well inside the research study values.

Secondly, many research studies in recent years have shown the greening of the Earth during the few last decades. Zhu et al. [23] have found a widespread increase of growing season integrated Leaf Area Index (LAI) (greening) over 25–50% of the global vegetated area, whereas less than 4% of the globe shows decreasing LAI (browning). Based on recent inventory data and long-term field observations, Pan et al. [24] have estimated that the global carbon sink between 1990 and 2007 has been 2.4±0.4 GtC yr⁻¹ in the terrestrial sink, meaning about 40.8 GtC from 1990 to 2017. Cheng et al. [25] have calculated that Earth's global terrestrial uptake has increased by 0.83±0.26 GtC per year, or a total of 24.9 GtC over the past three decades. Furthermore, they determined that a 10% increase in atmospheric CO₂ induces an approximate 8% increase in global gross primary production (GPP). Bastin et al. [26] have estimated that the global forest cover has increased about 9%, which is 40–47% more than previous estimates. They have increased the estimates of global forest carbon stocks by 15 to 158.3 GtC in comparison to that of Pan et al. [24]. Keenan et al. [27] have estimated that the residual carbon sink has steadily increased over recent decades from 1–2 GtC yr⁻¹ in the 1950s to 2–4 GtC yr⁻¹ in the 2000s. The latter figure is greater than the sink value of 2.5 GtC yr⁻¹ in 2017 per IDAOBM-3 simulation.

Estimates of the terrestrial sink show an essential growth, but the values still vary a lot. The calculated terrestrial sink value of 127 GtC since 1750 is on the high end of these estimates. The research studies show that the increase in

atmospheric CO₂ will also increase the global GPP production in the future.

Thirdly, the residence time of the anthropogenic CO₂ in the atmosphere is 16 years, the same as that of the radiocarbon ¹⁴C value, observed since

the nuclear bomb tests in 1964. The model-calculated total atmospheric CO₂ concentration correlates very well with the observed CO₂ concentration: the coefficient of determination is 0.999, and the standard error of estimate is 0.79 ppm during the period from 1960 to 2017.

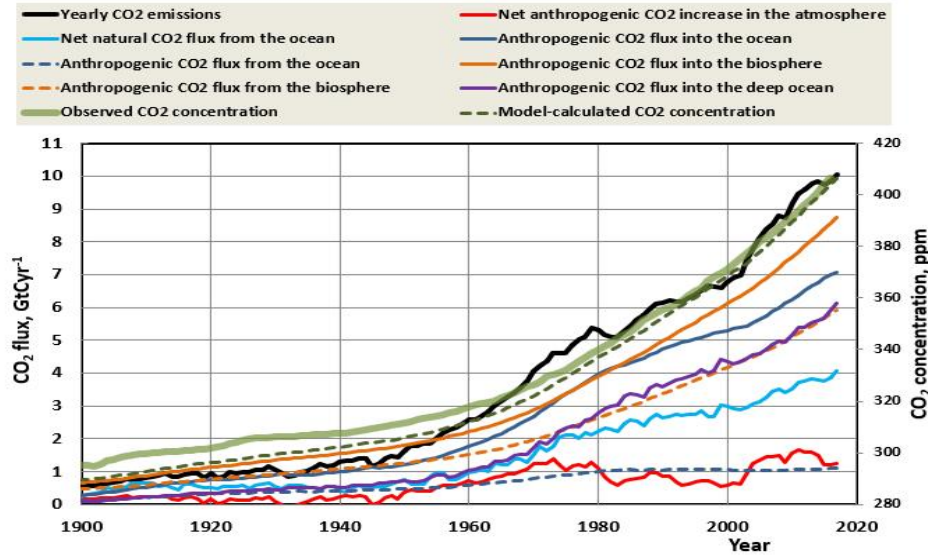


Fig. 2. Yearly CO₂ emissions and fluxes between the reservoirs by 1DAOBM-3 using the data as defined in section 2.1

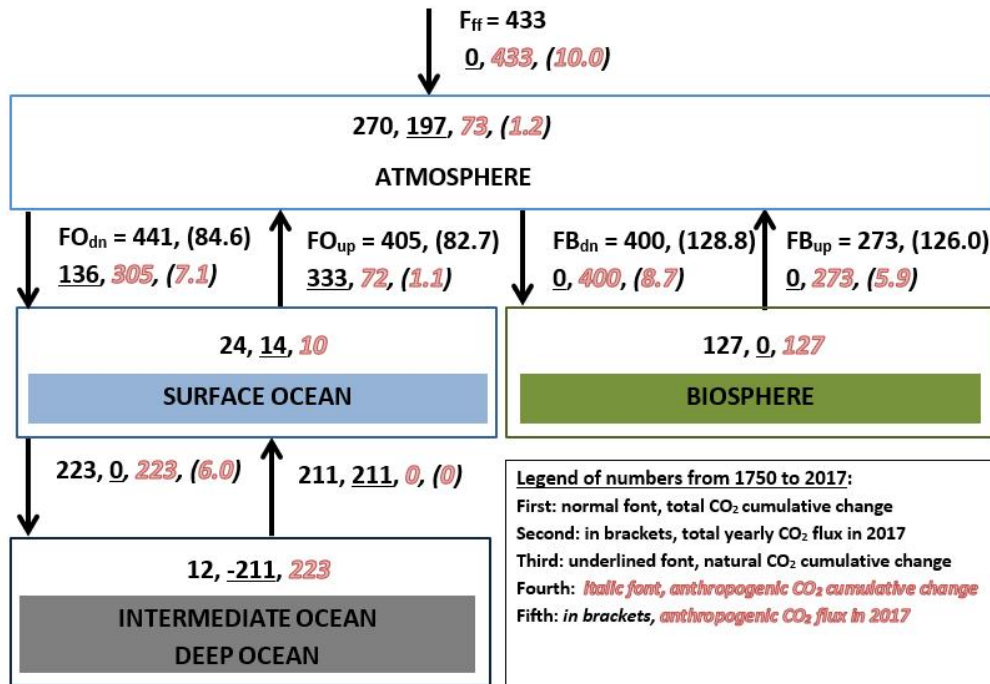


Fig. 3. The cumulative CO₂ flux changes and reservoir change values from 1750 to 2017

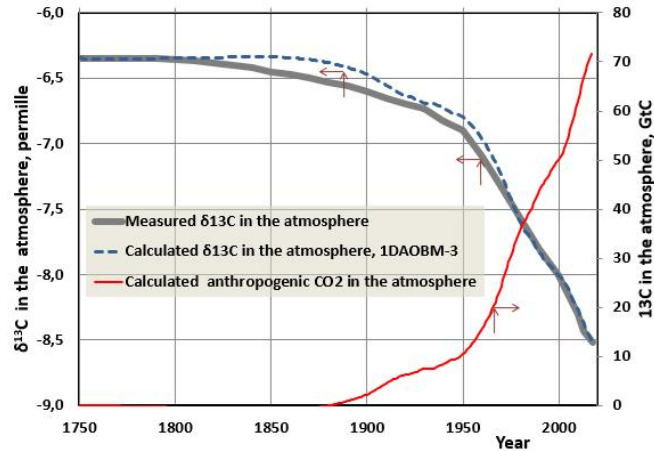


Fig. 4. Observed and 1DAOBM-3-calculated permille values in the atmosphere and the cumulative anthropogenic CO₂ value in the atmosphere from 1750 to 2017

Fourthly, the flux rate of anthropogenic CO₂ into the deep ocean has been calibrated according to the observed permille values of -8.56 for δ¹³C in 2017. The model-calculated permille trend value from 1750 to 2017 shows a very good fit with the observed value [7,9] as indicated in Fig. 4.

3. RESULTS

3.1 The Basic Features of the Bern2.5CC and Joos2013 Models

The carbon cycle model of Bern2.5CC [2] is a combination of a well-mixed atmosphere, the HILDA ocean model [28], and the Lund-Potsdam-Jena (LPJ) dynamic global vegetation model [29]. The HILDA model consists of two well-mixed surface boxes for low and high latitudes, a well-mixed deep-water box for high latitudes, a well-mixed atmosphere, and a vertically diffusive-advective ocean interior in low latitudes. The LPJ model combines process-based, large-scale representations of terrestrial vegetation dynamics and land-atmosphere carbon and water exchanges in a modular framework. The atmospheric CO₂ decay response C of a CO₂ pulse (In) according to time t can be fitted into a combination of three different residence times [1]

$$C = \ln * (0.217 + 0.186 * \exp(t/1.189) + 0.338 * \exp(t/18.51) + 0.259 * \exp(t/172.9)) \quad (3)$$

The Joos2013 model is a mean result of 15 different CO₂ circulation models [4]. The mean of the results was calculated for a 100 GtC pulse in 2010 when the atmospheric CO₂ concentration

was 389 ppm. The atmospheric CO₂ decay response C of this CO₂ pulse according to time t is fitted into a combination of three different residence times [4].

$$C = \ln * (0.2173 + 0.2763 * \exp(t/4.304) + 0.2824 * \exp(t/36.54) + 0.224 * \exp(t/394.4)) \quad (4)$$

Both equations (3) and (4) include a constant, which means that a relatively large portion of about 21.7% of any anthropogenic CO₂ emission will stay in the atmosphere forever. This means that, according to these models, the balance of CO₂ between the atmosphere and the ocean and terrestrial sink will never come near the preindustrial state. The simulations of the Joos2013 model include the warming effects of CO₂ according to the climate sensitivity of 3.0°C.

Both Bern2.5CC and Joos2013 have the same feature as a majority of CO₂ circulation models: for a 1000–2000 GtC pulse, the CO₂ fraction remaining in the atmosphere is 20–25% [30]. It should be noted that even though the models calculate the atmospheric CO₂ concentration, the research studies [2,4] use the expression “anthropogenic CO₂” remaining in the atmosphere.

3.2 Simulation Results of 1000 GtC Emission

BP [31] has estimated that oil reserves will be exhausted by 2066 and gas reserves by 2068 if the production and consumption continue at the present rates. Humanity has used fossil fuels totaling 433 GtC by 2017. The total amount of

1000 GtC for a future scenario is thus a pessimistic value for future total emissions. The author has composed a 1000 GtC scenario by keeping the yearly emissions at 10.2 GtC until 2048 and thereafter by decreasing yearly emissions linearly to zero by 2100.

A simulation of the 1000 GtC emission amount was carried out by 1DAOBM-3. In Fig. 5, flux rates are yearly values, and in Fig. 6, the flux rate values are cumulative. The temperature remains in the value of 2017 onward.

The maximum values of different variables are the following: the amount of total atmospheric CO₂ is 1027 GtC in 2089; the CO₂ concentration is 482 ppm in 2067; anthropogenic CO₂ in the atmosphere is 82.4 GtC in 2041; the natural CO₂ amount in the atmosphere is 379 GtC in 2089; and the anthropogenic CO₂ in the biosphere is 367 GtC in 2110. The latter value starts to decrease gradually, being 250 GtC in 2300, because 10% of a yearly anthropogenic CO₂ flux from the biosphere has a delay time of 80 years to return into the atmosphere.

It is rather difficult to estimate the net CO₂ rate change in the biosphere in Fig. 5. Therefore, this important variable has been depicted as a function of the atmospheric CO₂ concentration in Fig. 7.

Even though the CO₂ flux rate into the biosphere depends linearly on the CO₂ concentration, it turns out that the net rate change becomes nonlinear after 2023 when the CO₂ concentration exceeds 420 ppm, and in 2050 the net rate change does not increase anymore. The nonlinearity develops from 2023 to 2046 when the yearly emission rates are still at the constant values of 10.2 GtC. This nonlinearity has been caused by the CO₂ flux from the biosphere, when the delay times of 5, 20, 60 and 80 years from the root respiration develop into full effect according to Eq. (A23). Because after 2100 there are no CO₂ emissions anymore, the biosphere becomes a net source of CO₂ into the atmosphere after 2110.

The dynamic models of Bern2.55CC and Joos2013 are combinations of first-order dynamic processes. A dynamic first-order process can be simulated in the discrete form, enabling continuously changing input variables:

$$dT(n) = \Delta t / (T + \Delta t) / ((T / \Delta t) * (Out(n-1) + In(n)) \quad (5)$$

where Out(n) is the output of the process in step n, In(n) is the input of the process of step n, T is

the time constant, Δt is the simulation step interval (1 month), and n-1 is the previous step value. Fig. 8 depicts the CO₂ concentration of three CO₂ models according to the actual emissions.

All models overreact for the input change during the first 25-30 years. Thereafter the longest residence times of Bern2.55CC and Joos2013 control the output of these models, and the error in comparison to the observed CO₂ increases rapidly, being 432.5 ppm for Bern2.55CC and 441.5 ppm for Joos2013 in 2017, when the actual measured value is 406.5 ppm. The output of 1DAOBM-3 follows very well the observed CO₂ value being 407.3 ppm in 2017.

Fig. 9 depicts the CO₂ concentration curves of the Bern2.55CC and Joos2013 circulation models, and the fitted curve of the 1DAOBM-3 model. The fitting is according to a first-order dynamic process

$$C = 0.35 * \ln^*(\exp(t/12)) + 0.65 * \ln^*(\exp(t/150)) \quad (6)$$

where C is CO₂ concentration, \ln is the CO₂ emission input, and the time constants are 12 and 150 years.

The fitting curve for 1DAOBM-3 is not perfect, but it is simple and describes in an illustrative way how the sequestration rate decreases as the amount of CO₂ increases in the ocean and the terrestrial sink. In the simulation of Fig. 9, the outputs of the three models have been forced to the observed CO₂ value in 2010, even though the simulations start from 1950. This explains why the CO₂ concentration curves of Bern2.55CC and Joos2013 do not have the overreaction after 1950. Joos et al. [2] have used this kind of forcing in Bern2.55CC by starting the simulations from the observed CO₂ values in 1800 or 2000.

According to the 1DAOBM-3 simulation, the maximum CO₂ concentration will be 482 ppm in 2067, and it has decreased to 375 ppm in 2210. The decreasing rate of the atmospheric CO₂ in 143 years has been from 1027 GtC to 799 GtC corresponding to 0.75 ppm decrease per year, which means the average uptake rate of 1.6 GtC per year by the sinks. As Fig. 5 illustrates the deep ocean uptake rate is in the maximum value of 3.1 GtC⁻¹ in 2067. The maximum CO₂ concentration of Joos2013 is 567 ppm in 2087, and the value in 2210 is 518 ppm. The differences between 1DAOBM-3 and the other two models are significant.

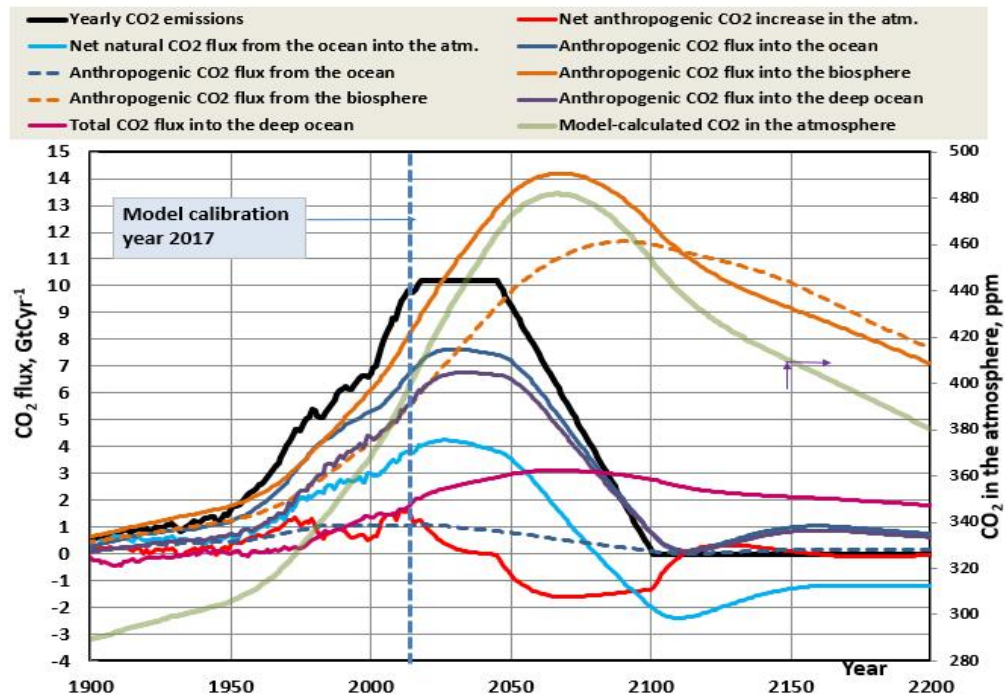


Fig. 5. Simulation result for a 1000 GtC emission by 1DAOBM-3 showing the yearly flux rates

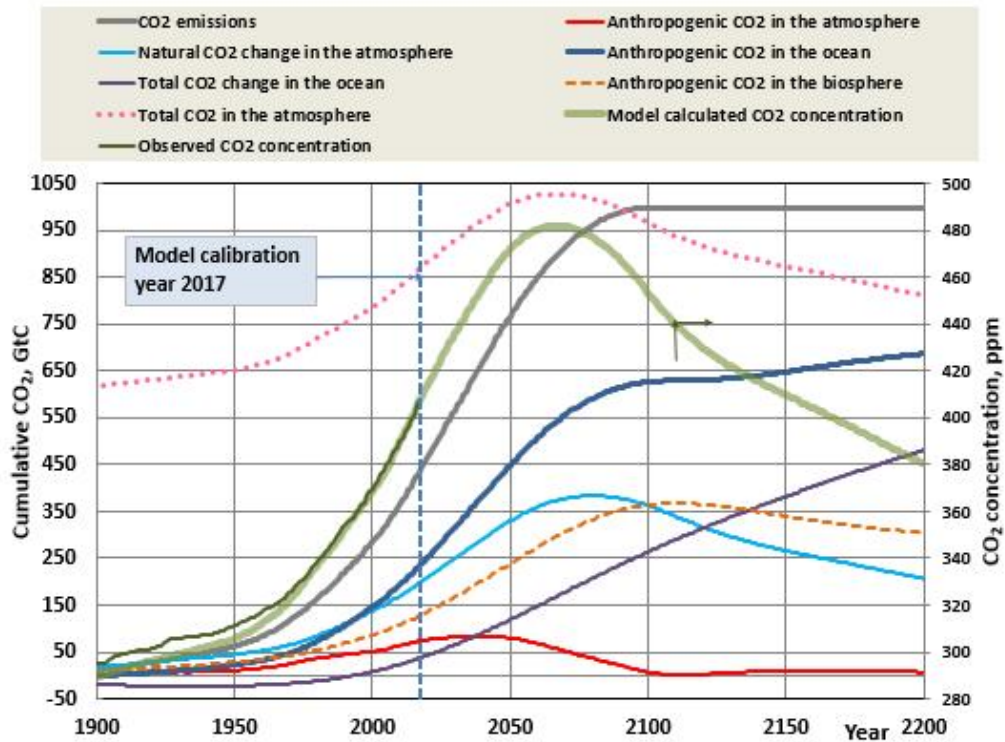


Fig. 6. Simulation result for a 1000 GtC emission amount by 1DAOBM-3 showing the cumulative flux rates

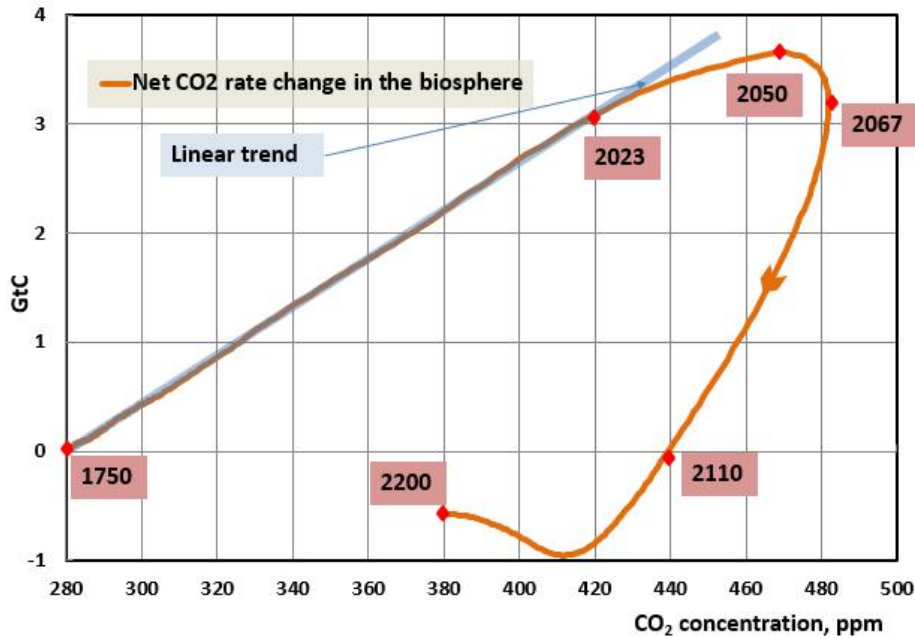


Fig. 7. Simulation result for a 1000 GtC emission amount by 1DAOBM-3 showing net CO₂ rate changes in the biosphere. The red dots show years

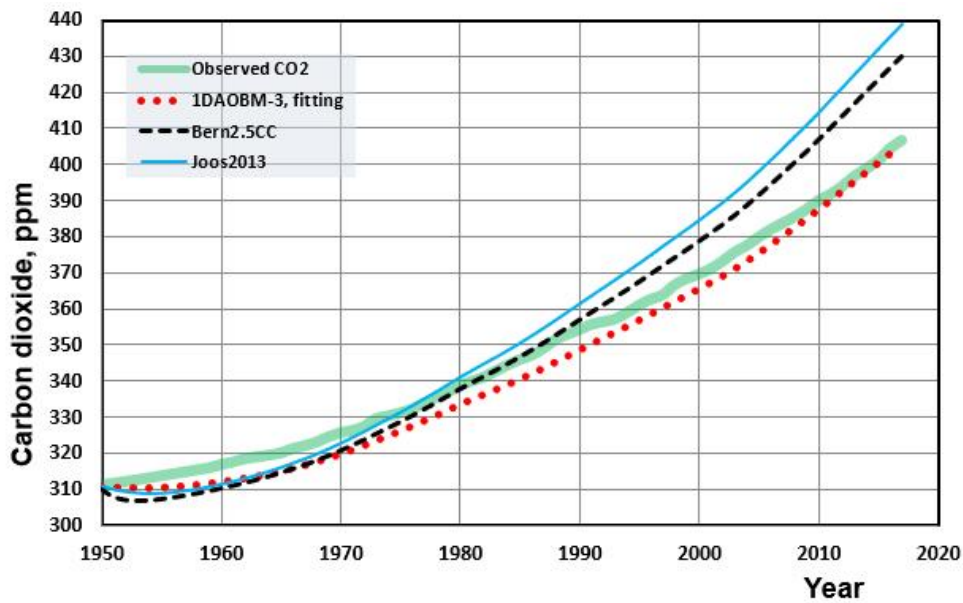


Fig. 8. The CO₂ concentration curves of three CO₂ circulation models according to actual CO₂ emissions from 1950 to 2017

Because the CO₂ concentration of Bern2.5CC and Joos2013 does not return close to the preindustrial value of 280 ppm after 1000 GtC emissions, the comparison based on the “end point” is not useful. A more realistic comparison point can be selected to be the conditions of the

year 2020 in Fig. 8, when the CO₂ concentration will be about 410 ppm. The statistical and scientific facts show that today’s climate conditions are better than in 1750, and therefore it is a proper reference point.

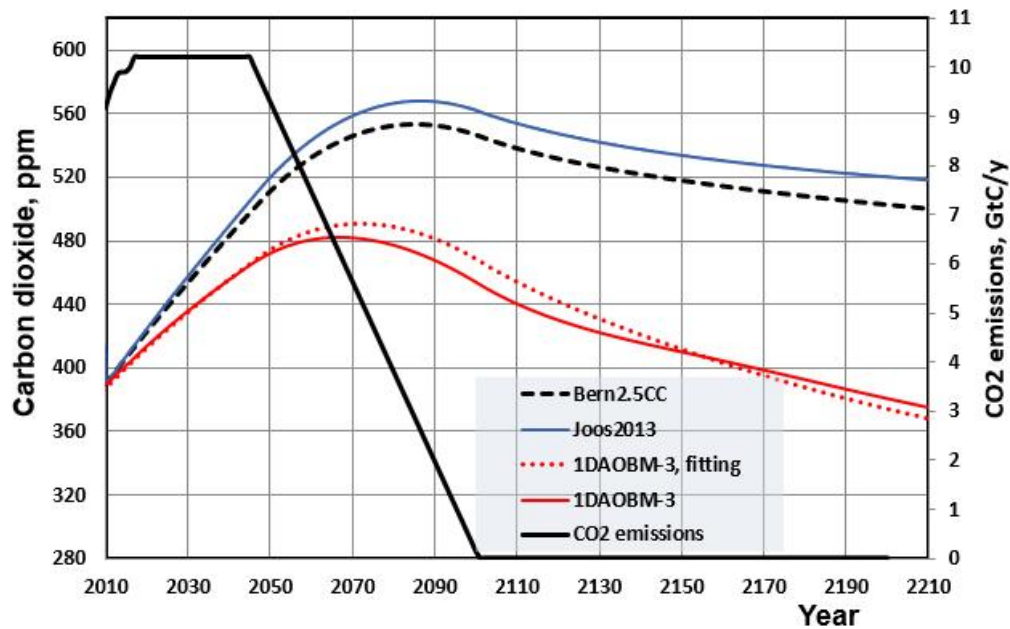


Fig. 9. The CO₂ concentration change of three CO₂ circulation models for the total 1000 GtC emissions from 1730 to 2100. The start year of simulations is 1950 but the model-calculated CO₂ concentrations are forced to the observed CO₂ concentration in 2010

The major concerns of the increased global temperature have been the increased amount of hazardous climate events and decreased crop amounts. The annual tornado account since 1954 shows that violent tornado frequency has been decreasing [32]. The landfall metric of Atlantic hurricanes reveals a statistically significant downward trend since 1950 [33]. A significant decrease in tropical and global cyclone frequencies has been observed since the late 1990s [34,35]. The world's wheat production has increased steadily, even in the warmest countries like India and Brazil [36]. India's government reports that food grain production was estimated to be at an all-time high in 2016–2017 [37] during the highest temperature peak during the present warm period.

The proxy temperature analyses reveal two warm periods [38], namely the Roman warm period from 250 BC to AD 450 and the Middle Age warm period from AD 950 to 1250. The retreating Mendenhall glacier in Alaska has exposed forest remnants older than 1,000 years based on their radiocarbon ages according to a statement by professor Connor [39]. Evidence shows that these warm periods, which have been called climate optimum periods, have been long

and at least as warm as the present one. According to the evidence, we are living again in climate optimum conditions.

3.4 Simulation Results of Decay Times

The easiest way to compare these three models is to depict the decay rates. Fig. 10 depicts the decay rates according to the fitting equations (3), (4), (6), and (7) starting from 2010.

The fourth curve in Fig. 10 is for 1DAOBM-3 by using 70 years' residence time. It is represented as a reference to illustrate the effective residence time would be about 70 years after 70 years and then it increases gradually to 150 years. The major difference of 1DAOBM-3 model is that the CO₂ impulse rate decreases to almost zero after 300 years but the other two models show that about 22-30% of the impulse size is still in the atmosphere.

4. DISCUSSION

The grounds of the CO₂ circulation models are different. Bern2.5CC and Joos2013 are principally built on the assumptions that the buffer factor phenomenon restricts the maximum uptake of the ocean to 2.2–2.3 GtC per year. In

1DAOBM-3, there is no this kind of restriction but despite this, the net maximum uptake rate is only 3.1 GtC yr⁻¹ in a 1000 GtC emission simulation.

Because all three models utilize the measured anthropogenic values in the oceans in 1990–1994, this flux value into the deep ocean is about the same in 1990–1994 but not necessarily the same thereafter due to the maximum uptake rate of 2.3 GtC yr⁻¹ of Bern2.5CC and Joos2013. In 1DAOBM-3, the net anthropogenic CO₂ rate into the ocean is 6.1 GtC yr⁻¹, and the net natural CO₂ rate from the ocean into the atmosphere is 4.2 GtC yr⁻¹ in 2017. This means that the net CO₂ flux into the ocean is still only 1.9 GtC yr⁻¹, which is smaller than the buffer-restricted rate. It looks like other two models do not consider the natural CO₂ from the ocean into the atmosphere. The major consequence is that the anthropogenic CO₂ amount in the atmosphere of these models is far too great.

During the first 30 years, the calculated CO₂ concentrations by the Bern2.5CC and the Joos2010 models from 1950 to 2017 show too low values and relatively great error for the year 2017: 432.5 ppm and 441.5 ppm versus the observed 406.6 ppm. The output of 1DAOBM-3 closely follows the observed CO₂ value, being 406.5 ppm in 2017. The Bern2.5CC simulation in Fig. 2 of Joos et al. [2] closely follows the actual CO₂ concentration from 1800 to 2000 [40]. The simulation starting from 1950 in Fig. 8 shows that

the Bern2.5CC model calculated values start to deviate from the observed values after 30 years. The author cannot explain these different results, but it seems logical that Bern2.5CC and Joos2013 give higher atmospheric CO₂ concentration values in the long run due to the longer residence times, as seen in the decay curves in Fig. 8.

The situation in 2149 corresponds to the CO₂ concentration of 410 ppm in 2020 according to 1DAOBM-3. The carbon budget shows that the ocean has sequestered the total anthropogenic CO₂ of 647 GtC by 2167; the terrestrial sink value is 341 GtC, and the atmosphere has 11 GtC of the anthropogenic CO₂. The division between the oceanic and terrestrial sinks is thus 66% / 34% in 2167.

The buffer-restricted uptake of the ocean has a commonly accepted theory basis. In research studies before 2010, this led to the so-called “missing carbon” problem because the increased terrestrial sink was not generally accepted. This problem can be found in the missing sink by Bern2.5CC [2], in which the terrestrial sink is accepted as the missing sink surrogate before 2000, which then turns into the CO₂ source. In research studies after 2000, the terrestrial sink has been accepted as reality. For example, according to Canadell [41], 5 GtC of 9 GtC emissions in 2006 have been taken up naturally, half by the ocean and half by the terrestrial biosphere.

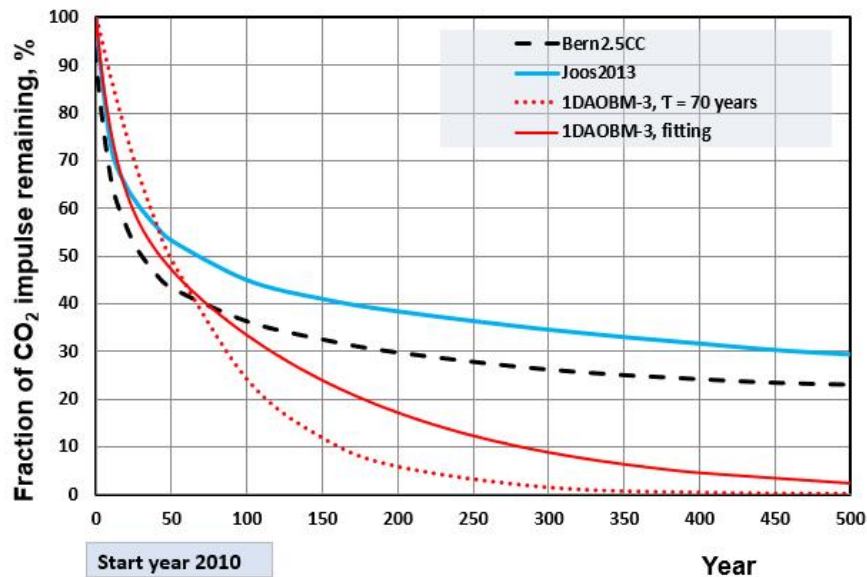


Fig. 10. Decay rates of atmospheric CO₂ concentration using different carbon cycle models

But there could be another mechanism that could explain a 35% greater maximum uptake rate of 3.1 GtC yr^{-1} per 1DAOBM-3 versus 2.3 GtC yr^{-1} . The CO_2 sequestration by the ocean in 1DAOBM-3 is based on the ocean circulation fluxes between the atmosphere and the ocean. The dissolving flux varies between $75\text{--}90.7 \text{ GtC yr}^{-1}$, and the absorbing flux from the ocean varies between $75\text{--}87.7 \text{ GtC yr}^{-1}$. These flux rates have been calibrated according to the measured atmospheric anthropogenic and total CO_2 amounts in 2017. The actual cold ocean circulation currents, which transfer the CO_2 -rich seawater from the high latitudes (mainly the North Atlantic) into the Southern Ocean, are not very well known concerning their rates and interactions with the deep ocean. It is generally accepted that the cold ocean waters dissolve CO_2 from the atmosphere, and thereafter, these cold ocean currents flow toward the Southern Ocean, where the warmer sea water absorbs CO_2 back into the atmosphere.

Archer and Brovkin [30] have stated that the dissolved CO_2 must wait for the overturning circulation of the ocean, which takes centuries or a millennium. These time scales are not well known. It could be assessed on the basis of the speeds of warm surface currents like the Gulf current. Its speed is estimated to be about 4 km per hour, so it would take about 3 months for the Gulf current to flow from Key West to the Arctic Ocean. This huge water mass flow cannot disappear, but it must continue flowing below the surface, and it does so as a Labrador current and an East Greenland Current. These cold currents flow at depths of 2000–4000 thousand meters, and they flow to the south as the Canary Current up to the Equator. If the water mass of these currents is close to the Gulf current, the time from the Arctic Ocean to the Equator should be months, not centuries. One example of time scales is that the atmospheric CO_2 concentration reacts with an 11-month delay to the Ocean temperature change [42].

The uptake process of CO_2 by the ocean is complicated and there might be doubts that the oceanic anthropogenic CO_2 could be different by nature in comparison to the same in the atmosphere. All the researchers who have carried out the estimation studies of the anthropogenic oceanic CO_2 amounts or fluxes have not identified this problem but they inform that the oceanic anthropogenic CO_2 can be summarized into the total mass of fossil fuel

emissions distributed in atmospheric, oceanic and terrestrial sinks as noticed in the review article [22].

Keeling et al. [43] have found that land photosynthesis increases the discrimination of ^{13}C isotopes when the atmospheric CO_2 concentration increases. They propose a correction term of $+0.014\text{‰ ppm}^{-1} \pm 0.007\text{‰ ppm}^{-1}$ for the model-calculated atmospheric permille values if these values are based on the land photosynthesis model. When this correction term is applied for the results of Joos2013 model, the calculated permille value of -12.9‰ in section 1 would increase to -11.2‰ . 1DAOBM-3 was calibrated using the observed atmospheric permille value in 2017 and therefore the possible increased ^{13}C discrimination of land photosynthesis has been included in the model. It should be noticed that the carbon residence time in terrestrial vegetation is one of the major uncertainties in the future climate responses [44].

Major uncertainties of 1DAOBM-3 are the deep-sea sequestration rate and the terrestrial uptake rate of carbon. Both models are linear depending on the CO_2 concentration of surface ocean or the atmospheric CO_2 concentration, but it turns out the net rate change in the biosphere becomes highly nonlinear after the CO_2 concentration of 420 ppm. The calibration of model parameters depends on atmospheric permille value. In this way 1DAOBM-3 model is in line with the observed values in 2017, when cumulative CO_2 emissions have been 433 GtC. The future uptake rate of the biosphere includes uncertainties because the model equations are simple and possible saturation or nonlinear effects of higher CO_2 concentrations are not included.

A pessimistic estimate for the total CO_2 of humanity is 1000 GtC. If a model is in line with the observations at the point of 43% of the possible scale, it is a good possibility that the model works well during the rest of the scale. The net uptake of the ocean has been only 36 GtC of total CO_2 by 2017, and the sequestration capacity of the ocean has not been utilized almost at all. The photosynthesis rate dependency on the CO_2 concentration for C3 plants is close to linear in the concentration from 280 to 600 ppm. Increasing biomass also increases humidity and rain conditions regionally and these factors are positive indicators that also terrestrial uptake rate could continue to increase in a linear way in the future.

5. CONCLUSION

As analyzed in section 1, the Bern2.5CC and Joos2013 models include a serious problem with the amount of anthropogenic CO₂ in the atmosphere: Joos2013 shows the anthropogenic CO₂ to be 240 GtC in 2011, when the direct permille measurement shows that the value is 67 GtC. This “wrong carbon” error in the atmospheric composition of Bern2.5 and Joos2013 models leads to another significant error. The mechanism of CO₂ circulation flows does not recognize that there is a great net natural CO₂ flux from the ocean into the atmosphere since 1750.

1DAOBM-3 calculates that the anthropogenic CO₂ in the atmosphere in 2017 is only 73 GtC. This CO₂ amount produces a calculated permille value of -8.52‰, practically the same as what was observed. Also, the historical permille values are close to the observed values. Because the total amount of atmospheric CO₂ in the same year was 867 GtC, the missing portion is natural CO₂, which must originate from the ocean, and its amount is 198 GtC, as shown in Fig. 2.

The big difference in 1DAOBM-3 in comparison to the other two models is that there are much greater anthropogenic and natural fluxes between the atmosphere and the ocean, as in the buffer-limited approach, but the net flux is not much greater. The result is that the 1DAOBM-3 approach can explain how the natural CO₂ enters the atmosphere, and it satisfies all the observed values of the atmospheric measurements, but the buffer-restricted approach cannot do it.

The cumulative values of 1DAOBM-3 from 1750 to 2017 show that the total (anthropogenic + natural) CO₂ in the ocean since 1750 has hardly started to increase because its amount as depicted is only 36 GtC. The ocean sink amount means only a 1.9% increase in the total oceanic CO₂, which is a very small increase considering the terrestrial sink increase in recent decades. This means that the uptake capacity of the oceans has not been practically utilized at all by 2017.

COMPETING INTERESTS

Author has declared that no competing interests exist.

REFERENCES

1. IPCC. Fourth Assessment Report (AR4). The physical science basis, contribution of

working Group I to the Fourth Assessment Report of the intergovernmental panel on climate change, Cambridge University Press, Cambridge; 2007.

2. Joos F, Prentice IC, Sitch S, Meyer R, Hooss, et al. Global warming feedbacks on terrestrial carbon uptake under the Intergovernmental Panel on Climate Change (IPCC) emission scenarios. *Glob. Biogeochem. Cycles*. 2001;15:891–908.
3. IPCC. Fifth Assessment Report (AR5). The physical science basis. Working Group I contribution to the IPCC fifth assessment report of the intergovernmental panel on climate change, Cambridge University Press, Cambridge; 2013.
4. Joos F, Roth R, Fuglestedt JS, Peters GP, Enting IG, et al. Carbon dioxide and climate impulse response functions for the computation of greenhouse gas metrics: A multi-model analysis. *Atmos. Chem. Phys*. 2013;13:2793–2825.
DOI: 10.5194/acp-13-2793-2013
5. Ollila A. Timescales of anthropogenic and total carbon dioxide (CO₂) in the atmosphere. *Phys. Sc. Int. J*. 2016;11(3):1-19.
6. NOAA. The data: What ¹³C tells us. The global view; 2018a.
Available:<http://www.esrl.noaa.gov/gmd/outr each/isotopes/c13tellsus.html>
7. Archer D, Brovkin V. The millennial atmospheric lifetime of anthropogenic CO₂. *Clim. Chang*. 2008;90:283–297.
DOI: 10.1007/s10584-008-9413-1
8. Böhm F, Haase-Schramm A, Eisenhauer A, Dullo W-C, Joachimski MM, et al. Evidence for preindustrial variations in the marine surface water carbonate system from coralline sponges. *Geochem. Geophys. Geosyst*. 2002;3(3).
DOI: 10.1029/2001GC000264
9. Inoue H, Sugimura Y, Fushimi K. pCO₂ and ¹³C in the air and surface sea water in the Western North Pacific. *Tellus*. 1987;39B: 228-242.
10. Scripps. Graphs Gallery. Global Stations Isotopic ¹³C Trends; 2018.
Available:http://scrippsco2.ucsd.edu/graphic s_gallery/isotopic_data/global_stations_isoto pic_13c_trends
11. Revelle R, Suess H. Carbon dioxide exchange between atmosphere and ocean and the question of an increase of

- atmospheric CO₂ during past decades. *Tellus*. 1957;9:18-27.
12. Gruber N, Gloor M, Mikaloff Fletcher SE, Doney SC, Dutkiewicz S, et al. Oceanic sources, sinks, and transport of atmospheric CO₂. *Glob. Biogeochem. Cycles*. 2009;23: GB1005.
DOI: 10.1029/2008GB003349
 13. Graven HD, Gruber N, Key R, Khatiwala S, Giraud X. Changing controls on oceanic radiocarbon: New insights on shallow-to-deep ocean exchange and anthropogenic CO₂ uptake. *J. Geophys. Res.* 2012;117: C10005.
DOI: 10.1029/2012JC008074
 14. Khatiwala S, Primeau F, Hall T. Reconstruction of the history of anthropogenic CO₂ concentrations in the ocean. *Nature*. 2009;462:346–349.
 15. Butler JN. Carbon dioxide equilibria and their applications. Addison-Wesley Publishing Company, New York. 1982;259.
 16. Maier-Reiner E, Hasselmann K. Transport and storage of CO₂ in the ocean - an inorganic ocean-circulation carbon cycle model. *Clim. Dyn.* 1987;2:63-90.
 17. Stumm W, Morgan JJ. Aquatic chemistry. An introduction emphasizing chemical equilibria in natural waters. John Wiley & Sons, New York; 1970.
 18. Ollila A. Anthropogenic carbon dioxide (CO₂) amounts and fluxes between the atmosphere, the ocean, and the biosphere. *Phys. Sc. Int. J.* 2015;8(1):1-17.
 19. CDIAC. Carbon emission from 1750 to 2013; 2018.
Available:http://cdiac.ornl.gov/ftp/ndp030/global.1751_2010.ems
 20. NOAA. Ocean temperature data base; 2018b.
Available:<ftp://ftp.ncdc.noaa.gov/pub/data/ml/ost/operational/products/>
 21. Sabine CL, Feely RA, Gruber N, Key RM, Lee K, et al. The oceanic sink for the anthropogenic CO₂. *Science*. 2004; 305(5682):367–371.
 22. Waugh DW, Hall TM, McNeil BI, Key R, Matear RJ. Anthropogenic CO₂ in the oceans estimated using transit time distributions. *Tellus Ser. B.* 2006;58:376–389.
 23. Sabine CL, Tanhua T. Estimation of anthropogenic CO₂ inventories in the ocean. *Annual Rev. Mar. Sci.* 2009;2:175–198.
DOI:10.1146/annurev-marine-120308-080947
 24. Zhu Z, Piao S, Myneni RB, Huang M, Zeng Z, et al. Greening of the earth and its drivers. *Nat. Clim. Chang*; 2016.
DOI: 10.1038/nclimate3004.
 25. Pan Y, Birdsey RA, Fang J, Houghton R, Kauppi PE, et al. Large and persistent carbon sink in the world's forests. *Science*. 2011;333(6045):988-93.
DOI: 10.1126/science.1201609
 26. Cheng L, Zhang L, Wang Y-P, Canadell JG, Chiew FHS, et al. Recent increases in terrestrial carbon uptake at little cost to the water cycle. *Nat. Comm.* 2017;8:110.
 27. Bastin J-F, Berrahmouni N, Grainger A, Maniatis D, Mollicone D, et al. The extent of forest in dryland biomes. *Science*. 2017;356: 635-638.
DOI: 10.1126/science.aam6527
 28. Keenan T, Prentice IC, Canadell JG, Williams CA, Wang H, et al. Recent pause in the growth rate of atmospheric CO₂ due to enhanced terrestrial carbon uptake. *Nat. Comm.* 2016;7:13428.
DOI: 10.1038/ncomms13428
 29. Shaffer G. Effects of the marine biota on global carbon cycling, in *The Global Carbon Cycle*, NATO ASI series, edited by M Heimann. Springer-Verlag Berlin Heidelberg. 1993;431–455.
 30. Sitch S, Smith B, Prentice IC, Arneth A, Bondeau A, et al. Evaluation of ecosystem dynamics, plant geography and terrestrial carbon cycling in the LPJ dynamic global vegetation model. *Glob. Chang. Biol.* 2003;9(2):161-185.
 31. Archer D, Brovkin V. The millennial atmospheric lifetime of anthropogenic CO₂. *Clim. Chang.* 2008;90:283–297.
DOI: 10.1007/s10584-008-9413-1
 32. BP World reserves of fossil fuels; 2017.
Available:<https://knoema.com/smsfgud/bp-world-reserves-offossil-fuels>
 33. NOAA. Historical trends and records of tornadoes; 2018c.
Available:<https://www.ncdc.noaa.gov/climate-information/extreme-events/us-tornado-climatology/trends>
 34. Trachelut RE, Staeling EM. An energetic perspective on united states tropical cyclone landfall droughts. *Geo. Res. Lett.* 2017;44(23):12013-12019.
 35. Zhao H, Wu L, Raga GB. Inter-decadal change of the lagged inter-annual relationship between local sea surface temperature and tropical cyclone activity over the Western North Pacific. *Theor. Appl. Clim.* 2018;134(1-2):707–720.

36. Maue RN. Recent historically low global tropical cyclone activity. *Geo. Res. Lett.* 2011;38:L14803.
Available:<https://doi.org/10.1029/2011GL047711>.
37. FAOSTAT. Production quantities of wheat in world; 2017.
Available:<http://www.fao.org/faostat/en/#data/qc/visualize>
38. Livemint. Foodgrain production estimated at a record 272 million tonnes in 2016-17.govt; 2017.
Available:<http://www.livemint.com/Politics/f2etZiWEzUq4I4J490UjM/Record-272-million-tonnes-food-grains-in-201617-agricultur.html>
39. Lungqvist FC. A new reconstruction of temperature variability in the extra-tropical Northern Hemisphere during the last two millennia. *Geogr. Ann. Ser. A-phys.Geogr.* 2010;92(A3):339–351.
40. Connor C. Statement, Richard Dawkins Foundation, Ancient forest thaws from melting glacial tomb; 2013.
Available:<https://richarddawkins.net/2013/09/ancient-forest-thaws-from-melting-glacial-tomb-livescience/>
41. Keeling CD, Piper SC, Bacastow RB, Wahlen M, Whorf TP, et al. Exchanges of atmospheric CO₂ and ¹³CO₂ with the terrestrial biosphere and oceans from 1978 to 2000. I. Global aspects, SIO Reference Series, No. 01-06, Scripps Institution of Oceanography, San Diego, 2001;88.
Available:http://scrippsco2.ucsd.edu/data/atmospheric_co2/icecore_merged_products
42. Canadell JG, Quere CL, Raupach MR, Field CB, Buitenhuis ET, et al. Contributions to accelerating atmospheric CO₂ growth from economic activity, carbon intensity, and efficiency of natural sinks. *Proc. Natl. Acad. Sci. USA.* 2007;104(24):10288–10293.
43. Humlum O, Stordahl K, Solheim J-E. The phase relation between atmospheric carbon dioxide and the global temperature. *Glob. Planet. Change.* 2013;100:51-69.
Available:<https://www.sciencedirect.com/science/article/pii/S0921818112001658>
44. Keeling RF, Graven HD, Welp LR, Resplandy L, Bi J, et al. Atmospheric evidence for a global secular increase in carbon isotopic discrimination of land photosynthesis. *PNAS.* 2017;114:10361-10366.
Available:www.pnas.org/cgi/doi/10.1073/pnas.1619240114
45. Friend AD, Lucht W, Rademacher TT, Keribin R, Betts R, et al. Carbon residence time dominates uncertainty in terrestrial vegetation responses to future climate and atmospheric CO₂. *PNAS.* 2014;111:3280–3285.
Available:www.pnas.org/cgi/doi/10.1073/pnas.1222477110
46. Sarmiento JL, Gruber N. Ocean biogeochemical dynamics. Princeton University Press, Princeton, NJ, USA; 2006.
47. Still CJ, Berry JA, Collatz J, DeFries RS. *Glob. Change Biol.* 2003;17:6-16-14.
48. Taiz L, Zeiger E. *Plant physiology.* Redwood City, Benjamin/Cummings Publishing Company; 1991.
49. Leakay ADB, Xua F, Gillespiea KM, McGratha JM, Ainswortha EA, Ort DR. Genomic basis for stimulated respiration by plants growing under elevated carbon dioxide. *PNAS.* 2009;106(9):3597-3602.
Available:<https://doi.org/10.1073/pnas.0810955106>
50. Gonzalez-Meler MA, Taneva L, Trueman RJ. Plant respiration and elevated atmospheric CO₂ concentration: Cellular responses and global significance. *Annals of Botany.* 2004;94:647–656.
Available:<https://doi.org/10.1093/aob/mch189>

APPENDIX

Table A-1. The calculation bases for variables and coefficients of the 1DAOBM-3. The amounts are in GtC and fluxes are in GtC yr⁻¹

Variable Acronym	Variable name	Calculation formula
FO _{tot,dn}	Total dissolution carbon pump flux from the atmosphere into the ocean	$80.5 + K_{dn} * (CIA - CIA_{1750})$; $K_{dn} = 0.0366$; CIA is the total atmospheric carbon (1)
FLUSH _{AO} -%	Flush-% of the dissolution pump from the atmosphere into the ocean	$100 * FO_{tot,dn} / CIA_{tot,n}$ (2)
FO _{ant,dn}	Anthropogenic dissolution carbon pump flux from the atmosphere into the ocean	$FLUSH_{AO}\% * CIA_{ant,n-1} / 100$ (3)
FO _{nat,dn}	Natural dissolution carbon pump flux from the atmosphere into the ocean	$FO_{tot,dn} - FO_{ant,dn}$ (4)
FO _{tot,up}	Total dissolution carbon pump flux from the ocean into the atmosphere	$80.5 + K_{up} * (CSO_{tot} - CSO_{1750})$; $K_{up}=0.32$ (5)
FLUSH _{OA} -%	Flush-% of the dissolution pump from the ocean into the atmosphere	$100 * FO_{tot,up} / CSO_{tot,n}$ (6)
FO _{ant,up}	Anthropogenic dissolution carbon pump flux from the ocean into the atmosphere	$FLUSH_{OA}\% * CSO_{ant,n-1} / 100$ (7)
FO _{nat,up}	Natural dissolution carbon pump flux from the ocean into the atmosphere	$FO_{tot,up} - FO_{ant,up}$ (8)
ΔCIA _{nat}	Natural net CO ₂ flux change from the ocean into the atmosphere	$FO_{nat,up} - FO_{nat,dn}$ (9)
CSO _{tot}	Dissolved organic carbon in the ocean in the range of 280 ppm – 430 ppm	$2.2 - 5.5774 * 10^{-3} * T - 8.631 * 10^{-5} * T^2 + 6 * 10^{-4} * (C-350)$; T is ocean temperature (°C), C is CO _{2,tot} concentration in CSO (10)
CSO _{tot}	Dissolved organic carbon in the ocean in the range of 430 ppm – 600 ppm	$2.255 - 5.114 * 10^{-3} * T - 6.84 * 10^{-5} * T^2 + 3 * 10^{-4} * (C-500)$; T is ocean temperature (°C), C is CO _{2,tot} concentration in (11)
FN _{ant,deep}	Anthropogenic net CO ₂ flux from the surface ocean into the intermediate & deep ocean	$K_{ant} * (CSO_{tot,n} - CSO_{tot,1750}) * (CSO_{ant,n-1} / CSO_{tot,n})$; $K_{ant} = 16.0$ (12)
ΔCSO _{tot}	Total CO ₂ change in the surface ocean	$CSO_{tot} - CSO_{tot,1750}$ (13)
ΔCSO _{ant}	Anthropogenic CO ₂ change in the surface ocean	$FO_{ant,down} - FO_{ant,up} - FN_{ant,deep}$ (14)
ΔCSO _{nat}	Natural CO ₂ change in the surface ocean	$ΔCSO_{tot} - ΔCSO_{ant}$ (15)
FN _{ant,ocean}	Anthropogenic CO ₂ flux into the ocean	$FN_{ant,deep} + ΔCSO_{ant}$ (16)
FN _{nat,deep}	Net natural CO ₂ flux from the deep ocean	$FO_{nat,atm} - ΔCSO_{nat}$ (17)
FN _{tot,deep}	Total net CO ₂ flux into the deep ocean	$FN_{ant,deep} + FN_{nat,deep}$ (18)
ΔCDO _{ant}	Anthrop. CO ₂ change in the deep ocean	$F_{deep,n} - F_{deep,n-1}$ (19)
FB _{tot,dn}	Total biosphere carbon cycle flux from the atmosphere into the	$120 + KB_{dn} * (CIA - CIA_{1750})$; $KB_{dn} = 0.017$ (20)

Variable Acronym	Variable name	Calculation formula	
	biosphere		
FLUSH _{AB} -%	Flush-% of the biosphere carbon cycle from the atmosphere into the biosphere	$100 * FB_{tot,dn} / CIA_{tot,n}$	(21)
FB _{ant,dn}	Anthropogenic biosphere carbon cycle flux from the atmosphere into the biosphere	$KA_{dn} * CIA_{tot,n-1}$ $KA_{dn} = 0.03305$	(22)
FB _{ant,up}	Anthropogenic biosphere carbon cycle flux from the biosphere into the atmosphere	$0.5 * CIA_{tot,n-1} + 0.1 * CIA_{tot,n-5} + 0.05 * CIA_{tot,n-20}$ $+ 0.2 * CIA_{tot,n-60} + 0.1 * CIA_{tot,n-80}$	(23)
ΔCIB_{ant}	Anthrop. CO ₂ change in the biosphere	$FB_{ant,down} - FB_{ant,up}$	(24)
ΔCIA_{ant}	Anthrop. CO ₂ change in the atmosphere	$F_{ff} - \Delta CSO_{ant} - \Delta CDO_{ant} - \Delta CIB_{ant}$; F_{ff} is CO ₂ emission flux	(25)
ΔCIA_{tot}	Total CO ₂ change in the atmosphere	$\Delta CIA_{nat} + \Delta CIA_{ant}$	(26)
F _{ff}	Anthropogenic CO ₂ emission flux from fossil fuel combustion		

Total dissolution carbon pump flux from the atmosphere into the ocean $FO_{tot,dn}$ depends linearly on the difference of the atmospheric CO₂ amount minus the same in 1750 per eq. (A1). As a consequence, $FO_{tot,dn}$ increases from 75.0 GtCyr⁻¹ in 1750 to 84.62 GtCyr⁻¹ in 2017. Total dissolution carbon pump flux from the ocean into the atmosphere $FO_{tot,up}$ depends linearly on the difference of the surface ocean total CO₂ concentration minus the same in 1750 per eq. (A5). As a consequence, $FO_{tot,up}$ increases from 75.0 GtCyr⁻¹ in 1750 to 82.72 GtCyr⁻¹ in 2017. The linear dependencies of eq. (1A) and eq. (5A) means that both fluxes increase as the total atmospheric CO₂ increases, and both fluxes diminish into the 1750 value if the actual CO₂ concentration values in the atmosphere or in the surface ocean approach the values of the year 1750. The IPCC (2011) has used the values of Sarmiento and Gruber [45], which are 60 GtCyr⁻¹ in 1750 and 80.0 GtCyr⁻¹ in 2011. The dependency on the atmospheric CO₂ concentration is thus smaller in this study.

The coefficient K_{ant} is 16.0 in eq. (A12) and is calibrated so that the amount of atmospheric anthropogenic CO₂ gives permille values of -8.56 for $\delta^{13}C$ in 2017. Coefficients K_{dn} and K_{up} have been calibrated so that the natural cumulative CO₂ amount in the atmosphere is 197 GtC from 1750 to 2017 closing the total CO₂ amount in the atmosphere in 2017. The total CO₂ change in the ocean is only 36 GtC from 1750 to 2017. A major change is that that the total biosphere carbon flux $FB_{tot,dn}$ from the atmosphere into the biosphere depends linearly on the atmospheric CO₂ per eq. (A20).

The CO₂ flux into the biosphere $FB_{ant,dn}$ increases linearly on the increasing total atmospheric CO₂ concentration (Eq. A22). This is an approximation of the photosynthesis rate for C4 plants which represent 82% vegetated land surface [46]. The actual rate is slightly nonlinear for C4 plants [47] and for C3 plants it is about constant after 350 ppm. Because the CO₂ concentration exceeded 350 ppm in 1987, the error not including C3 plants in the model is rather small. The increase in biomass increases also other important growing conditions like humidity and rains in regional scale. In the earlier model version, it depended on the anthropogenic CO₂ amount. The coefficients KB_{dn} and KA_{dn} have been calibrated so that the CO_{2,ant} of the biosphere in 2017 is 127 GtC, thus closing the CO_{2,ant} budget in different reservoirs.

The respiration of plants happens in leaves and roots in relationship roughly 50%/50%. The research studies of the respiration rate of plants in elevated CO₂ concentrations show contradicting results. For example Drake [48] found that CO₂ respiration decreased about 10% in high higher CO₂ concentrations, and Leakey et al. [49] found that respiration increased 37% in 550 ppm concentration. Gonzalez-Meler et al. [50] have concluded that respiration rate stays about at constant value in the elevated CO₂ conditions. Decreasing respiration means greater take up rate. There is no

generally accepted research result concerning respiration dependency on CO₂ concentration. It should be noticed that respiration studies have been short term studies related to respiration process in leaves. The long term respiration models are almost non-existing. Therefore, the CO₂ flux from the biosphere into the atmosphere (Eq. 20)) has not been revised, because there is no reliable new research studies about the respiration rate.

© 2019 Ollila; This is an Open Access article distributed under the terms of the Creative Commons Attribution License (<http://creativecommons.org/licenses/by/4.0>), which permits unrestricted use, distribution, and reproduction in any medium, provided the original work is properly cited.

Peer-review history:

*The peer review history for this paper can be accessed here:
<http://www.sdiarticle4.com/review-history/53980>*